

Performing high-quality multi-photon experiments with parametric down-conversion

This article has been downloaded from IOPscience. Please scroll down to see the full text article.

2009 J. Phys. B: At. Mol. Opt. Phys. 42 114008

(<http://iopscience.iop.org/0953-4075/42/11/114008>)

[The Table of Contents](#) and [more related content](#) is available

Download details:

IP Address: 131.130.45.80

The article was downloaded on 09/04/2010 at 11:16

Please note that [terms and conditions apply](#).

Performing high-quality multi-photon experiments with parametric down-conversion

Thomas Jennewein¹, Rupert Ursin^{1,2}, Markus Aspelmeyer¹ and Anton Zeilinger^{1,2}

¹ Institut für Quantenoptik und Quanteninformation, Österreichische Akademie der Wissenschaften, Boltzmannngasse 3, 1090 Wien, Austria

² Fakultät für Physik, Universität Wien Boltzmannngasse 5, 1090 Wien, Austria

Received 12 December 2008, in final form 9 February 2009

Published 15 May 2009

Online at stacks.iop.org/JPhysB/42/114008

Abstract

We demonstrate entanglement swapping of polarization entangled photons using an interferometric Bell-state measurement operating at the theoretical limit of 50% efficiency capable of identifying two of the four Bell states. Our experiment represents the highest quality of entanglement swapping so far, with the correlations of the final entangled states showing an overlap fidelity with the ideal Bell states of $F = 0.892$, and a violation Bell's inequality for both swapped entangled states. In order to achieve this high-quality operation we have optimized various experimental error sources of our setup including the quality of optical elements, as well as the constraints due to the coherence and the group-velocity mismatch of the pump and down-conversion photons. Our results are relevant for experiments that involve interferences of independent photons and pulsed multi-photon states, such as in quantum computing, quantum metrology and quantum communication with quantum repeaters.

(Some figures in this article are in colour only in the electronic version)

1. Introduction

Quantum state teleportation [1] allows the transfer of an unknown quantum state from one system to an independent system, without obtaining any information on the quantum systems. This protocol has been demonstrated with polarized photons [2], as well as with squeezed quadratures of light [3], with ions [4, 5], liquid-state nuclear magnetic resonance [6] and between atoms and light [7, 8]. A fascinating case of quantum teleportation is entanglement swapping, where the transferred state is not only unknown but undefined, since it is part of an entangled pair. According to quantum mechanics, the entanglement perfectly sustains this procedure [9], which has also been shown in experiments [10–13] by the violation of a Bell inequality [14] for particles that never interacted. Entanglement swapping and teleportation are important protocols for linear optical quantum computing [15] schemes, where essentially the generalization of entanglement swapping is a crucial element for achieving scalable operations and the fusion of large entangled states from smaller initial states [16]. Entanglement swapping is also at the heart of

quantum repeater protocols [17], which aim at extending distances of quantum entanglement by concatenating and purifying entanglement to cover large distances. Furthermore, the methods of entanglement swapping are also important for fundamental tests of entanglement between massive particles, such as single trapped atoms [12, 18]. Here, achieving the long distances required for an ultimate and loophole free Bell test (see [19] for a review) will require high-quality entanglement swapping schemes.

The standard protocol for quantum state teleportation relies on two key resources which are the entanglement of particles and an entangling operation, called the Bell-state analysis (BSA). When using qubits, there are four possible entangled Bell states describing the possible quantum correlations between them. With linear optical elements it is only possible [20] to detect two of the four Bell states perfectly. Such an optimal linear optics Bell-state analysis for entangled photon pairs was demonstrated experimentally in quantum dense coding experiments [21, 22], and in quantum teleportation [23], and recently in an entanglement swapping

experiment [11]. It was shown theoretically by Kwiat *et al* [24] and later in experiment [25], that by exploiting hyper entangled photons a seemingly four-state BSA is possible, but this scheme is not applicable to quantum teleportation or entanglement swapping.

Here we present the realization and optimization of entanglement swapping based on an optimal Bell-state analyser, capable of detecting two of the four Bell states. Our setup allowed us to observe that correlations between the swapped entangled photons violated Bell's inequality separately for each of the two possible Bell states obtained in the BSA. In this work, we will in particular study the effects of various experimental factors that reduce the attainable entanglement swapping quality. Consequently we will observe the overlap fidelity of the final entangled states with the ideal states, and test the Bell inequality as a witness for entanglement.

2. Experimental setup

Our setup is shown in figure 1. Two entangled photon pairs a, b and c, d are generated by spontaneous parametric down conversion (SPDC) in a barium-borate crystal (BBO) [26], pumped by ultraviolet laser pulses with a wavelength of 395 nm and 200 fs pulse width. All photons are sent through narrowband bandpass filters, with a full width at half-maximum (FWHM) bandwidth of 3 nm for the outer photons, and 1–2 nm for the inner photons. These two inner photons b and c are interfered on the BSA, whereas the two outer photons are separately analysed and detected. The BSA was realized by interfering the two photons b and c first on a 50:50 fibre beam splitter (BS), and with additional polarizers (PBS) in each of the output arms of the BS. The detection of the two Bell states was performed as follows: when a photon was found in each output arm of the beam splitter BS, and in opposite outputs of their polarizers, then a $|\Psi^-\rangle_{bc}$ -Bell state was observed (either detectors D1H and D2V fire, or D1V and D2H). However, if the two photons were found in the same output arm of the beam splitter, but in different outputs of the polarizer, then a $|\Psi^+\rangle_{bc}$ -Bell state was observed (either D1H and D1V fire, or D2H and D2V).

It is interesting to note that this two-outcome-BSA allows performing entanglement swapping optimized in a more general sense. One would naively expect that the teleportation of entanglement works equally well for all four Bell states in the case that these are non-maximal entangled. Yet, Bose *et al* [27] were able to show that two of the four Bell states will experience a purification in their final entanglement, whereas the other two Bell states will become even less entangled, which was also shown experimentally [28]. The consequence of this insight is that practical entanglement swapping experiments would not necessarily lead to a huge advance when even a full Bell-state analyser is implemented.

The two-photon interference performed within this BSA required full compensation of the polarization rotation in all the fibres, which was a rather tedious and timely process. However, once good alignment was achieved, the polarization in the fibres was stable to about 5° over 24 h. The rate of

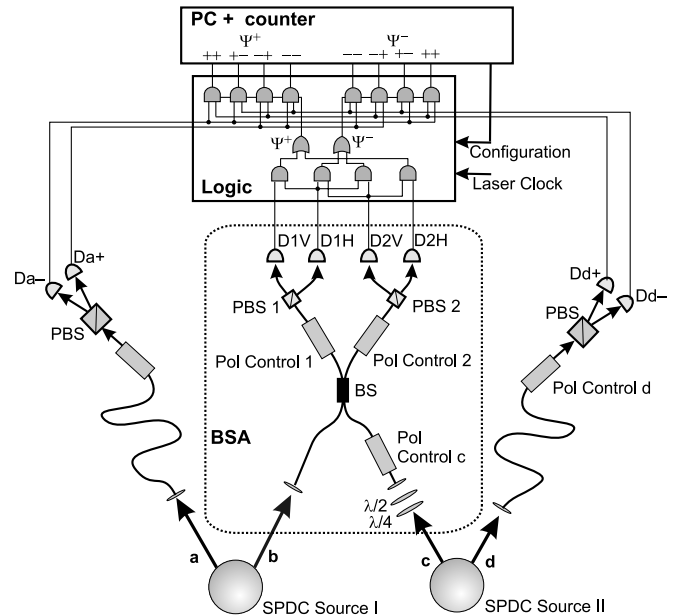


Figure 1. Setup of entanglement-swapping experiment using optimal Bell-state analysis. The two photon pairs are produced by spontaneous parametric down conversion [47] in barium-borate pumped by UV-laser pulses (wavelength = 394 nm, width = 200 fs, rate = 76 MHz). From the two entangled photon pairs (pair $a-b$, and pair $c-d$), one photon each (photons b and c) is sent to the Bell-state analyser, consisting of a 50:50 fibre beam splitter (BS) and with polarizing beam splitters in each output arm. The temporal overlap between photons b and c is adjusted by moving a mirror for the UV-pulses. The remaining photons a and d are separately analysed with polarizers (PBS) and detected in each output of the PBS. The spurious birefringence of the fibres which induces polarization rotations of the photons is compensated with polarization controllers. For the fibre beam splitter, also an additional half-wave plate ($\lambda/2$) and quarter-wave plate ($\lambda/4$) are used for the compensation of the phase between the reference polarization states. A coincidence logic, sketched with Boolean AND and OR gates, compares all eight detector signals and identifies the useful events of the four photons. The logic was realized in a programmable logic array [48]. The occurrences of the eight possible four-fold events were counted in a PC counter-card. The logic also included an adjustment mode for counting the twofolds and the singles count rates (configured from the PC).

entanglement swapping events achieved in this setup was about once every 2.5 min. Therefore counts were accumulated over measurement runs of at least 10 000 s per data point. One of the largest experimental challenges of this experiment was to achieve the entanglement swapping operation with such high level of quality, that the resulting entangled photons can violate Bell's inequality, a suitable test for the presence of quantum entanglement. Given the limited count rates, it was necessary to achieve a correlation visibility of the final entangled photons of better than $V \geq 0.80$, well above the limit of $V_{\text{thresh}} = \frac{1}{\sqrt{2}}$ required for violation of the Bell inequality [14, 29].

The expected contributions of all the above discussed effects are described in the appendix and summarized in table 1. In our experiment we performed a range of test measurements in order to compare the experimentally attainable two-photon interference (HOM) visibilities with the estimated visibilities, as will be discussed below. The

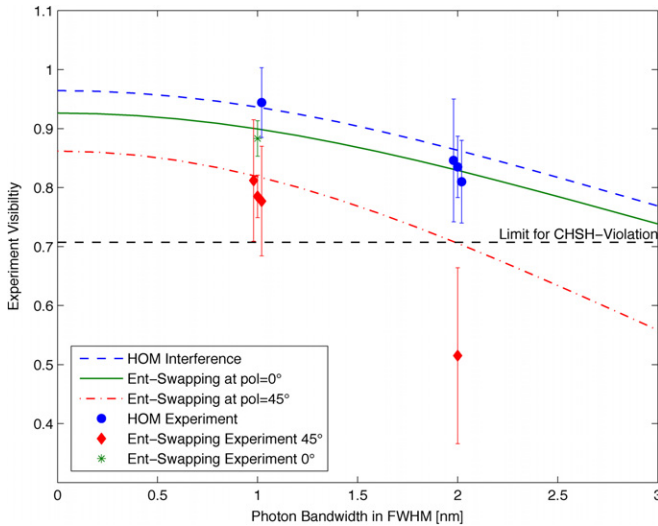


Figure 2. Measured two-photon interference visibilities compared with the calculation of our model, for three experimental scenarios. First, the Hong–Ou–Mandel interference (HOM) is considered, where the two photons b and c interfere at the beam splitter, and polarizers at 45° are placed in both of their paths. Second, an entanglement swapping experiment, where the correlation between photons a and d is observed with polarizers at 45° setting. Third, again an entanglement swapping experiment, but both the polarizers are oriented at 0°. Some measurements show larger error bars than the final results presented in table 2, since they were taken just for alignment purposes within a shorter experimental duration.

Table 1. Summary of the estimated visibility for the entanglement swapping experiments. See the text for details.

Filter bandwidth FWHM		1 nm	2 nm
Effect			
Two-fold correlation at 0°	$V_{I,0^\circ}$	0.980	0.980
Two-fold correlation at 45°	$V_{I,45^\circ}$	0.935	0.904
Splitting-ratio of the fibre BS	$V_{II,45:55}$	0.996	0.996
Polarization alignment in the fibres	$V_{IV,3^\circ}$	0.998	0.998
Center wavelength of photons b and c	$V_{V,0.25\text{nm}}$	0.977	0.977
Distinguishability of photons in HOM	V_{VI}	0.997	0.991
Temporal jitter between photon pairs	V_{VII}	0.964	0.881
Final swapping visibility at 0°	V_{0°	0.896	0.815
Final swapping visibility at 45°	V_{45°	0.816	0.693

measured results are shown in figure 2 and are compared with the estimation from our model which includes various sources of errors. With these insights it is possible to understand the limitation of the experimental quality of multi-photon experiments based on parametric down-conversion. More importantly, these estimations show that in our situation it is necessary to choose the filter bandwidth as narrow as 1 nm FWHM to finally achieve a level of entanglement well above the classical limits.

3. Optimization of the entanglement swapping quality

In the following, we give a detailed overview of the various effects limiting the quality for the interference of photons

coming from different pulsed SPDC processes. Each effect will be assigned with a visibility, and mostly defined as usual as $V = (C_{\max} - C_{\min}) / (C_{\max} + C_{\min})$, where C are the counted photon signals fringing between a maximal and minimal value. There is the exception for the case of the two-photon interference (Hong–Ou–Mandel dip), where the visibility must be measured as $V = (C_{\text{inf}} - C_{\text{min}}) / C_{\text{inf}}$, where C_{inf} are the counted two-photon events well outside the interference range, and C_{min} are the minimal counted events at the point of optimal interference (dip). In the first approximation, we estimate the total expected correlation visibility as the product of all the individual visibilities, $V_{\text{tot}} \simeq \prod_i V_i$.

3.1. Two-fold visibility of pulsed SPDC

First we consider the attainable quality of the two-fold correlations of the entangled photon pairs. An obvious source of error is the alignment accuracy of the polarizing optical elements in the down-conversion system (such as the SPDC crystals, the compensator crystals, wave plates [26]). In addition it has already been shown in several theoretical calculations and in experiments [30–34] that the in SPDC pumped with femtosecond laser pulses the achievable quality of two-fold entanglement is inherently reduced. Therefore the correlation visibility for measurements along the 45° or the circular polarization basis will have less quality than measurements in the 0° basis. In this experiment we observed in the 0°/90° polarization basis a visibility of $V_{I,1\text{nm},0^\circ} = 0.980$, and in the 45° basis, corresponding to a two-fold correlation visibility of $V_{I,1\text{nm},45^\circ} = 0.935$ with filters for photons b and c having a 1 nm FWHM bandwidth, and a visibility of $V_{I,2\text{nm},45^\circ} = 0.904$ with filters of 2 nm.

3.2. The Bell-state analyser

Since we are utilizing a fibre-optic beam splitter at the heart of the Bell-state analyser, the mode overlap is inherently perfect. As the only source of error we must take into account that the required splitting ratio of 50:50 is not perfectly achieved. The non-ideal splitting ratio leads to an achievable visibility of the two-photon interference of [35] $V_{II} = \frac{2RT}{R^2+T^2}$, with reflectivity R and transmittivity T . Our actual device had a splitting ratio of about 45:55, which reduced the visibility of the HOM interference by $V_{II,45:55} = 0.996$.

3.3. Higher order emission terms of SPDC

The emission characteristics of our photon pair production implies a similar probability for producing two photon pairs in separate modes (one photon each in modes a, b, c, d) or two pairs in the same mode (two photons each in modes a and b or in modes c and d). The latter events lead to ‘false’ coincidences in the detectors in the BSA hence creating a noise background. However, our optimal Bell-state analyser partially diminishes this problem, since it reduces the unwanted higher order events by at least a factor of 2. We exclude part of these cases by only accepting events where one photon each in modes a and d is registered. Furthermore, the Bell-state analyser will only detect a valid event when the two photons (b and c) take

separate H , V outputs of the polarizing beam splitters arranged behind the first beam splitter. In strongly pumped situations the higher order photon emissions from the SPDC can create a substantial amount of background, as was shown in detail in a recent study [36]. However, in our experiment we operated in a regime where the pair production rate was about 10^{-4} per pulse, hence the rate of false events was about 10^{-8} and was safely neglected.

3.4. Polarization alignment in the fibres

The quality of the polarization alignment of the two input fibres of the beam splitters is also a relevant parameter. Including a polarization rotation of $\Delta\phi$ for one of the inputs in the calculation of the interference leads to a visibility $V = \cos(\Delta\phi)$. In this experiment the two inputs of the beam splitter were aligned better than $\Delta\phi = 3^\circ$, as described above in figure 1. This results in a visibility limit of $V_{V,3^\circ} = 0.998$.

3.5. Frequency distinguishability of photons b and c

Obviously, any difference in the centre wavelengths of photons b and c interfering at the beam splitter makes them distinguishable [35], hence reducing the visibility of the HOM interference. This situation is described as $V_V = e^{-\frac{(\omega_{\text{diff}}\tau_{\text{cohr}})^2}{8}}$, where ω_{diff} is the difference in angular frequency of the two input wave packets and τ_{cohr} is their coherence time. A more practical expression can be found by expressing the coherence time in terms of the wavelength bandwidth, $\tau_{\text{cohr}} \approx 0.4247\lambda^2/(2\pi c\Delta\lambda_{\text{FWHM}})$, and the frequency difference in terms of the wavelength difference, $\omega_{\text{diff}} \approx 2\pi c\lambda_{\text{diff}}/\lambda^2$, leading to

$$V_V \approx e^{-0.3606\left(\frac{\Delta\lambda_{\text{diff}}}{\Delta\lambda_{\text{FWHM}}}\right)^2}, \quad (1)$$

where $\Delta\lambda_{\text{diff}}$ is the difference of the peak wavelengths of the wave packets and $\Delta\lambda_{\text{FWHM}}$ is their full width at half-maximum width of the spectral distribution. In our experiment $\Delta\lambda_{\text{FWHM}}$ was 1 nm, and the accuracy of the central wavelength of the filters was better than 0.25 nm. This resulted in a visibility of $V_{V,0.25\text{nm}} = 0.977$.

3.6. Timing distinguishabilities of photons b and c

With the finite bandwidths of the pump photons and the interfering photons there is a fundamental reduction of the HOM visibility for the interference of the independent photons, b and c. (In the ideal case, the pump photons would have an infinitely short pulse width which corresponds to an infinite spectral width.) The relation for the effect of timing on the lower bound for the HOM visibility was shown by Zukowski *et al* [9], and later generalized by Kaltenbaek *et al* [37] including the bandwidth of both SPDC photons and a synchronization jitter of the pump laser. The expression for the resulting visibility reads

$$V_{VI} = \frac{\sigma_p}{2\sqrt{\frac{(\sigma_b^2+\sigma_c^2)(\sigma_b^2+\sigma_c^2)}{\sigma_b^2+\sigma_c^2+\sigma_p^2}} - \sigma_p}, \quad (2)$$

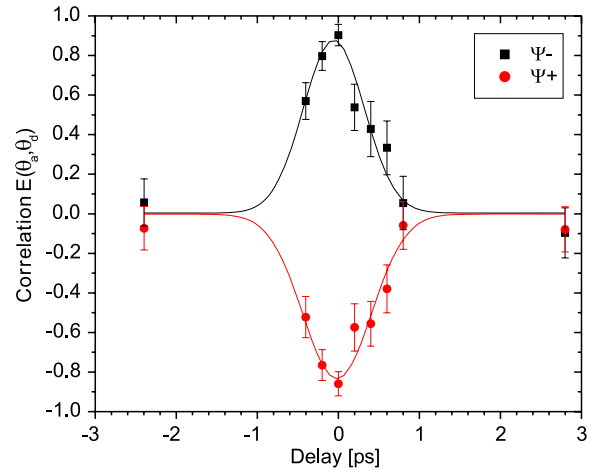


Figure 3. Measurement of the correlation coefficients for photons a and d, depending on the relative delay of photons b and c interfering in the Bell-state analyser. The setting of the polarizers was $\theta_a = \theta_d = 45^\circ$. The maximal correlation occurs for the optimal temporal overlap of the two wave packets of photons b and c. The two correlations were obtained in the same measurement by sorting the detection events corresponding to the outcome of the Bell-state measurement.

where σ_p , σ_i and σ_o are the 1σ widths for the respective Gaussian spectral distributions of the pump, the interfering photons and the outer photons. In our experiment for the case that the FWHM bandwidth of filters for photons b and c are 1 nm, this results in $V_{VI,1\text{nm}} = 0.997$, and in the case of 2 nm $V_{VI,2\text{nm}} = 0.991$.

3.7. Group-velocity mismatch of the down-conversion and pump photons

The origin of this effect is the group-velocity walk-off in the nonlinear crystal which leads to an inherent visibility reduction for the two-photon interference in pulsed down-conversion. When photons b and c from independent down-conversion processes are brought together for interference, their wave packets will experience a timing offset due to this speed difference between the pump and the down-conversion light. The extreme cases are that one photon pair is produced right at the beginning of the crystal and the second pair right at the end of the crystal, and vice versa. This is due to the dispersion properties of the BBO crystal, which has a temporal walk-off between the UV-pump photons, experiencing group delays of $u_{\text{pump}} = 5694 \text{ fs mm}^{-1}$, and the two down-conversion photons, propagating with group velocities $u_{\text{signal}} = 5413 \text{ fs mm}^{-1}$ and $u_{\text{idler}} = 5612 \text{ fs mm}^{-1}$, respectively [38]. The difference between the group velocities of the pump photons and the average of the SPDC photons is about $\Delta u = 180 \text{ fs mm}^{-1}$.

In order to estimate the resulting visibility due to the group velocity mismatch of pump and the SPDC photons, we varied the relative creation times of the photon pairs $t_{a,b}(x)$ and $t_{c,d}(x)$ over the position x along the crystal. Hence $t_{a,b}(x)$ can have any value in the range of $\pm d\Delta u/2$, where d is the thickness of the SPDC crystal. Assuming that all values of $t_{a,b}$ are equally likely, we integrate over the crystal length for both

photon pairs and obtain the overall two-photon coincidence probability as

$$P'_{b,c}(\tau) = \frac{1}{d^2} \int_{-d/2}^{d/2} \int_{-d/2}^{d/2} P_{b,c}(t_{a,b} - t_{c,d} - \tau) dt_{a,b} dt_{c,d}, \quad (3)$$

where τ is the offset of the two arms of the photons to the beam splitter. We further assume that the photon wave-packets are a Gaussian shape with the width equal to the coherence time τ_{cohr} of the photons, which interfere with time delay τ and the offset $t_{a,b} - t_{c,d}$. Therefore the coincidence probability for the interference of two photons is

$$P_{b,c}(t_{a,b} - t_{c,d} - \tau) = \frac{1}{2} \left(1 - \frac{2V_{\text{VI}}}{1+V_{\text{VI}}} \exp\left(\frac{(t_{a,b} - t_{c,d} - \tau)^2}{\tau_{\text{cohr}}^2}\right) \right). \quad (4)$$

In our experiment the crystal had a thickness of $d = 2$ mm, hence the photon pairs are undefined within the range of $|t_{a,b}| \leq 180$ fs (large compared to the photon coherence $\tau_{\text{cohr}} = 775$ fs for 1 nm bandwidth filters). The HOM visibility is defined as $V_{\text{VII}} = (P'(\text{inf}) - P'(0))/P'(\text{inf})$. The explicit numerical calculation of the integral (3) for filter band widths of $\Delta\lambda_{\text{FWHM}}$ of 1 nm, 2 nm, 3 nm leads to the HOM visibilities of $V_{\text{VII},1\text{nm}} = 0.9641$, $V_{\text{VII},2\text{nm}} = 0.8817$, $V_{\text{VII},3\text{nm}} = 0.7778$ respectively. A further advanced calculation should also include the synchronization jitter of two pump lasers, and is given by Kaltenbaek [39].

The standard approach for minimizing or even avoiding the effects of this group velocity mismatch is to use narrow bandwidth filters and thereby extend their coherence time of the SPDC photons beyond the group velocity dispersion. Unfortunately this leads to a huge loss of the generated photons. This timing effect is finally resolved by utilizing particular crystals with well chosen or even specifically tailored group velocity properties, that do not require any filters for the SPDC and still achieve high-quality two-photon interference [40–43].

4. Experimental results

The expected contributions of all the above discussed effects are summarized in table 1. The total visibility is calculated by taking the product of all contributing visibilities. In our experiment we performed a range of test measurements in order to compare the experimentally attainable HOM visibilities with the estimated visibilities, these discussed above. The measured results are summarized in figure 2 and compared with the respective estimates. Note the very good agreement of the experiment with the calculation. Now it is possible to understand the various effects that reduce the experimental quality in our entanglement swapping experiment. More importantly we are able the adequately choose the filter bandwidth as 1 nm FWHM, such that all further measurements on the entanglement swapping are performed at the required quality of the experiment.

The correlations of the entangled photons are quantified by measuring the correlations between photons a and d with the expectation value for joint polarization measurements $E(\phi_a, \phi_d)$, where ϕ_a and ϕ_d are the polarizer setting for photons

a and d, respectively [44]. The correlation coefficients are defined as

$$E(\phi_a, \phi_d) = (N_{++}(\phi_a, \phi_d) - N_{+-}(\phi_a, \phi_d) - N_{-+}(\phi_a, \phi_d) + N_{--}(\phi_a, \phi_d)) / \sum N_{ij}, \quad (5)$$

where as usual the $N_{ij}(\phi_a, \phi_d)$ are the coincidence counts between the i -channel of the polarizer of photon a set at angle ϕ_a , and the j -channel of the polarizer of photon d set at angle ϕ_d . Each measurement run of the correlation coefficients $E(\phi_a, \phi_d)$ for photons a and d at settings $\phi_a = \phi_d = 45^\circ$ involved a scan through the relative time delay between the photons b and c by moving a mirror in the path of the pump laser for one of the SPDC sources, see figure 3. Clearly the dependence of the photon interference on the delay between the two photons can be observed and highlights the operation of the interferometric Bell-state analysis used in this entanglement swapping experiment. This measurement actually shows the very high correlation of the entangled photons after the entanglement swapping of $E = 0.91$ for the $|\Psi^-\rangle_{\text{ad}}$ and $E = 0.86$ for the $|\Psi^+\rangle_{\text{ad}}$.

Several such expectation values E were used to obtain measures for the state fidelity, defined as $F = \langle \Psi | \rho \rangle$. To see how this was done, first take the general definition of a two-qubit density matrix ρ

$$\rho = \frac{1}{4} \left(\sum_0^3 T_{mk} \sigma_m \otimes \sigma_k \right) \quad (6)$$

where T_{mk} are the expectation values $\text{Tr}\{\rho \sigma_m \sigma_k\}$ for a particular spin measurement, σ_0 is the identity and $\sigma_{1,2,3}$ are the Pauli matrices. We also consider the projectors of the two Bell states used in our experiment, which are $|\Psi^\mp\rangle\langle\Psi^\mp| = 0.25(1 - \sigma_1\sigma_1 \mp \sigma_2\sigma_2 \mp \sigma_3\sigma_3)$ and obtain the fidelity via the trace $F_{|\Psi^\mp\rangle} = \text{Tr}\{\rho|\Psi^\mp\rangle\langle\Psi^\mp|\}$, leading to

$$F_{|\Psi^\mp\rangle} = \frac{1}{4}[1 - T_{11} \mp T_{22} \mp T_{33}]. \quad (7)$$

This expression is experimentally easily accessible, since it only requires three different measurements and not the set of the nine measurements (combinations of the three basis settings on either photon) needed for performing a tomography of the state – which made a huge practical difference given the limited count rates of our experiment. In our case the axis of the Pauli matrices are identified with the polarization, where $\sigma_{1,2,3}$ correspond to analyser setting in the H, 45 and L polarization basis. Therefore the coefficients in the above expression for the fidelity are $T_{11} = E(\text{H}, \text{H})$, and likewise for the other polarization bases.

We have performed the correlation measurements on the swapped entangled photons which end up in the $|\Psi^-\rangle_{\text{ad}}$ or $|\Psi^+\rangle_{\text{ad}}$ depending on the outcome of the bell-state analyser, see table 2. These results lead to overlap fidelities of the swapped entangled photons with the ideal Bell states of $F_{|\Psi^-\rangle} = 0.892$ and $F_{|\Psi^+\rangle} = 0.879$ for states $|\Psi^-\rangle_{\text{ad}}$ and $|\Psi^+\rangle_{\text{ad}}$, respectively.

As a sufficient indication of the presence of entanglement we tested a Bell inequality, where the suitable version for experiments is the Clauser–Horne–Shimony–Holt (CHSH) variant [29], which has the following form:

$$S = |E(\phi'_a, \phi'_d) - E(\phi'_a, \phi''_d)| + |E(\phi''_a, \phi'_d) + E(\phi''_a, \phi''_d)| \leq 2. \quad (8)$$

Table 2. Measured correlation values for photons a and d for polarizer settings $\theta_a; \theta_d$, after the entanglement swapping protocol. The outcome of the Bell-state measurement on photons b and c determines the type of correlation to be a Ψ^- or Ψ^+ . The first three measurements show the high quality of the entangled state in the three bases. These measurements give us the very high state fidelity of $F = 0.892$ and $F = 0.879$. The following four measurements allow us to test the CHSH inequality. As the local realistic upper limit for S is 2, above results for both Bell states clearly violate the CHSH inequality. Note that the correlation coefficients for the two Bell states were measured within the same measurement run for a particular polarizer setting by sorting the data into corresponding subsets. The given errors are the statistical uncertainties due to photon counting. The differences in the correlation coefficients come from the higher correlation fidelity for analyser settings closer to 0° and 90° .

$E(\theta_a; \theta_d)$	$ \Psi^-\rangle_{ad} \Psi^-\rangle_{bc}$	$ \Psi^+\rangle_{ad} \Psi^+\rangle_{bc}$
$E(0^\circ; 0^\circ)$	-0.972 ± 0.0	-0.957 ± 0.0
$E(45^\circ; 45^\circ)$	-0.832 ± 0.0	0.771 ± 0.0
$E(L; L)$	-0.765 ± 0.0	0.789 ± 0.0
$E(0^\circ; 22.5^\circ)$	-0.61 ± 0.04	-0.55 ± 0.04
$E(0^\circ; 67.5^\circ)$	0.80 ± 0.04	0.60 ± 0.04
$E(45^\circ; 67.5^\circ)$	-0.64 ± 0.05	0.48 ± 0.05
$E(45^\circ; 22.5^\circ)$	-0.55 ± 0.05	0.67 ± 0.05
Bell-parameter S	2.60 ± 0.09	2.30 ± 0.09

It is straightforward to show that the prediction of quantum mechanics leads to $E^{\text{QM}}(\phi_a, \phi_d) = -\cos(2(\phi_a - \phi_d))$. With the settings chosen as $(\phi'_a, \phi'_d, \phi''_a, \phi''_d) = (0^\circ, 22.5^\circ, 45^\circ, 67.5^\circ)$ the maximal value of $S^{\text{QM}} = 2\sqrt{2}$, which clearly violates the limit of 2 imposed by inequality (8). The necessary series of correlation coefficients of photons a and d were measured, and are given in table 2. Note that the correlation coefficients for the two different Bell states were measured within the same measurement run for a particular polarizer setting by sorting the data into corresponding subsets depending upon the observed Bell state. Our results show clear violations of the Bell inequality with $S = 2.60 \pm 0.09$ for the $|\Psi^-\rangle_{ad}$ and $S = 2.30 \pm 0.09$ for the $|\Psi^+\rangle_{ad}$ Bell state. The lower value of S for $|\Psi^+\rangle_{ad}$ is due to the difficult polarization alignment of the output fibres of the beam splitter.

5. Conclusion

We demonstrate an entanglement swapping experiment using photons produced by spontaneous parametric down-conversion (SPDC) and an optimal Bell-state analyser with 50% efficiency, i.e. capable of detecting two of the four Bell states perfectly. Via a thorough analysis and optimization of the experimental errors in our system, we achieved a very high experimental entanglement correlation and tested the violation of two Bell inequalities on the swapped photons in the same experiment run. In addition, we showed that the final entangled Bell states had an observed state fidelity $F = 0.892$ and $F = 0.879$ with the respective ideal states $|\Psi^-\rangle_{bc}$ and $|\Psi^+\rangle_{bc}$. In particular, we studied the various deteriorating effects in the spontaneous parametric down conversion which are crucial for performing high-quality multi-photon experiments, and gave a simple model that allowed us to estimate the final

state fidelity. We consequently improved the experimental performance by carefully optimizing the several sources of errors. As the main experimental obstacle for SPDC systems we also estimated the group velocity mismatch between the pump and the down-conversion photons in the SPDC crystal in a simple mathematical model, and compared the calculations with several test experiments. These calculations also allowed us to understand why in our case the required bandpass filters for the interfering photons must be the narrow value of 1 nm FWHM. We note that finally the problem of the group velocity mismatch will be solved by cancelling the dispersion effects with advanced phase-matching methods [40–43]. The various effects of errors must be considered in most types of multi-photon experiments that rely on two-photon interference effects and are based on parametric down-conversion.

From the fundamental side it is interesting to note that the observed violations of the Bell inequalities in our entanglement swapping experiment drastically highlights the non-classical nature of entanglement, since the outcome of the Bell-measurement of the two inner photons b and c ($|\Psi^-\rangle_{bc}$ and $|\Psi^+\rangle_{bc}$) even determines the type of entanglement of the two outer photons a and d ($|\Psi^-\rangle_{ad}$ and $|\Psi^+\rangle_{ad}$) [45].

Since teleportation using a two-outcome Bell-state measurement is also one of the building blocks of linear-optical quantum gates [46], this experiment clearly represent an important step for linear-optical quantum information processing, the creation of multi-photon entangled states and quantum repeater protocols.

Acknowledgments

We thank M Zukowski, D Greenberger, C Brukner, T Rudolph, A White, M Barbieri and R Kaltenbaek for fruitful discussions on experimental and theoretical questions. This work has been supported by the Austrian Science Foundation (FWF) Project No. F1506 and F1520, and by the European Commission under the Integrated Project Qubit Applications (QAP) funded by the IST directorate and the DTO-funded U.S. Army Research Office.

References

- [1] Bennett C H, Brassard G, Crépeau C, Jozsa R, Peres A and Wootters W K 1993 *Phys. Rev. Lett.* **70** 1895
- [2] Bouwmeester D, Pan J-W, Mattle K, Eibl M, Weinfurter H and Zeilinger A 1997 *Nature* **390** 575
- [3] Furusawa A, Sorensen J L, Braunstein S L, Fuchs C A, Kimble H J and Polzik E S 1998 *Science* **282** 706
- [4] Riebe M *et al* 2004 *Nature* **429** 734
- [5] Barrett M D *et al* 2004 *Nature* **429** 737
- [6] Nielsen M A, Knill E and Laflamme R 1998 *Nature* **396** 52 (<http://dx.doi.org/10.1038/23891>)
- [7] Sherson J F, Krauter H, Olsson R K, Julsgaard B, Hammerer K, Cirac I and Polzik E S 2006 *Nature* **443** 557 (<http://dx.doi.org/10.1038/nature05136>)
- [8] Chen Y-A, Chen S, Yuan Z-S, Zhao B, Chuu C-S, Schmiedmayer J and Pan J-W 2008 *Nature Phys.* **4** 103
- [9] Zukowski M, Zeilinger A and Weinfurter H 1995 *Ann. NY Acad. Sci.* **755** 91
- [10] Jennewein T, Weihs G, Pan J-W and Zeilinger A 2002 *Phys. Rev. Lett.* **88** 017903

- [11] Kaltenbaek R, Prevedel R, Aspelmeyer M and Zeilinger A 2008 High-fidelity entanglement swapping with fully independent sources (<http://www.citebase.org/abstract?id=oai:arXiv.org:0809.3991>)
- [12] Matsukevich D N, Maunz P, Moehring D L, Olmschenk S and Monroe C 2008 *Phys. Rev. Lett.* **100** 150404 (<http://link.aps.org/abstract/PRL/v100/e150404>)
- [13] Yuan Z-S, Chen Y-A, Zhao B, Chen S, Schmiedmayer J and Pan J-W 2008 *Nature* **454** 1098
- [14] Bell J 1964 *Physics* **1** 195
- [15] Kok P, Munro W J, Nemoto K, Ralph T C, Dowling J P and Milburn G J 2007 *Rev. Mod. Phys.* **79** 135 (doi:10.1103/RevModPhys.79.135)
- [16] Browne D E and Rudolph T 2005 *Phys. Rev. Lett.* **95** 010501 (doi:10.1103/PhysRevLett.95.010501)
- [17] Briegel H-J, Dür W, Cirac J I and Zoller P 1998 *Phys. Rev. Lett.* **81** 5932
- [18] Volz J, Weber M, Schlenk D, Rosenfeld W, Vrana J, Saucke K, Kurtsiefer C and Weinfurter H 2006 *Phys. Rev. Lett.* **96** 030404
- [19] Genovese M 2005 *Phys. Rep.* **413** 319 (<http://www.citebase.org/abstract?id=oai:arXiv.org:quant-ph/0701071>)
- [20] Calsamiglia J and Lütkenhaus N 2001 *Appl. Phys. B* **72** 67
- [21] Mattle K, Weinfurter H, Kwiat P G and Zeilinger A 1996 *Phys. Rev. Lett.* **76** 4656
- [22] Michler M, Mattle K, Weinfurter H and Zeilinger A 1996 *Phys. Rev. A* **53** R1209
- [23] Ursin R, Jennewein T, Aspelmeyer M, Kaltenbaek R, Lindenthal M, Walther P and Zeilinger A 2004 *Nature* **430** 849
- [24] Kwiat P G and Weinfurter H 1998 *Phys. Rev. A* **58** R2623
- [25] Schuck C, Huber G, Kurtsiefer C and Weinfurter H 2006 *Phys. Rev. Lett.* **96** 190501
- [26] Kwiat P G, Waks E, White A G, Appelbaum I and Eberhard P H 1998 arXiv:quant-ph/9810003
- [27] Bose S, Vedral V and Knight P L 1999 *Phys. Rev. A* **60** 194
- [28] Zhao Z, Yang T, Chen Y-A, Zhang A-N and Pan J-W 2003 *Phys. Rev. Lett.* **90** 207901
- [29] Clauser J F, Horne M A, Shimony A and Holt R A 1969 *Phys. Rev. Lett.* **23** 880
- [30] Mattle K 1997 *PhD Thesis* Universität Innsbruck
- [31] Czeija G 2001 *Master's Thesis* Universität Wien
- [32] Keller T and Rubin M 1997 *Phys. Rev. A* **56** 1534
- [33] Pittman T B, Strekalov D V, Migdall A, Rubin M H, Sergienko A V and Shih Y H 1996 *Phys. Rev. Lett.* **77** 1917
- [34] Scarcelli G, Valencia A and Shih Y 2004 *Phys. Rev. A* **70** 051802 (<http://www.citebase.org/abstract?id=oai:arXiv.org:quant-ph/0409210>)
- [35] Weihs G 1994 *Master's Thesis* Universität Innsbruck
- [36] Weinhold T J, Gilchrist A, Resch K J, Doherty A C, O'Brien J L, Pryde G J and White A G 2008 arXiv:0808.0794
- [37] Kaltenbaek R, Blauensteiner B, Zukowski M, Aspelmeyer M and Zeilinger A 2006 *Phys. Rev. Lett.* **96** 240502 (doi:10.1103/PhysRevLett.96.240502)
- [38] Sandia National Laboratories 2007, Snlo software, v.41, (<http://www.sandia.gov/imrl/XWEB1128/xxtal.htm>)
- [39] Kaltenbaek R 2008 *PhD Thesis* Universität Wien
- [40] Mosley P J, Lundeen J S, Smith B J, Wasylczyk P, U'Ren A B, Silberhorn C and Walmsley I A 2007 Herald generation of ultrafast single photons in pure quantum states (<http://www.citebase.org/abstract?id=oai:arXiv.org:0711.1054>)
- [41] U'Ren A B, Erdmann R K, de la Cruz-Gutierrez M and Walmsley I A 2006 *Phys. Rev. Lett.* **97** 223602 (<http://www.citebase.org/abstract?id=oai:arXiv.org:quant-ph/0611018>)
- [42] Kim Y-H, Kulik S P and Shih Y 2001 *Phys. Rev. A* **63** 060301 (<http://www.citebase.org/abstract?id=oai:arXiv.org:quant-ph/0007067>)
- [43] U'Ren A B, Silberhorn C, Erdmann R, Banaszek K, Grice W P, Walmsley I A and Raymer M G 2005 *Laser Phys. Lett.* **15** 146 (<http://www.citebase.org/abstract?id=oai:arXiv.org:quant-ph/0611019>)
- [44] Aspect A, Grangier P and Roger G 1982 *Phys. Rev. Lett.* **49** 91
- [45] Greenberger D M, Horne M and Zeilinger A 2005 A bell theorem without inequalities for two particles, using efficient detectors (<http://www.citebase.org/abstract?id=oai:arXiv.org:quant-ph/0510201>)
- [46] Knill E, Laflamme R and Milburn G 2000 *Nature* **409** 46
- [47] Kwiat P G, Mattle K, Weinfurter H, Zeilinger A, Sergienko A and Shih Y 1995 *Phys. Rev. Lett.* **75** 4337
- [48] Jennewein T 2002 *PhD Thesis* Universität Wien